PHYSICAL REVIEW C VOLUME 35, NUMBER 5 MAY 1987

Doorway states induced by quantum recoils

B. G. Giraud
Service de Physique Théorique, Centre d'Etudes Nucléaires de Saclay, F-91191 Gif-sur-Yvette Cédex, France

S. Kessal
Université Scientifique et Technique Houari Boumedienne, Institut de Physique, El-Alia, Alger, Algérie

L. C. Liu
Isotope and Nuclear Chemistry Division, Los Alamos National Laboratories, Los Alamos, New Mexico 87544
(Received 7 May 1986)

A proper treatment of the Pauli principle is usually impossible in Jacobi coordinate representation when heavy nuclei are involved; hence a shell-model representation of the collision becomes mandatory. This raises the traditional problems of shell-model spurious states and recoil corrections. We show how recoil parameters can actually be used as dynamical parameters in collision theories.

I. INTRODUCTION

Consider a system of N nucleons with momenta $\mathbf{p}_i$, $i=1,\ldots,N$, kinetic energies t_i, two-body interactions w_{ij}, and a structureless projectile with momentum $\mathbf{p}_0$, kinetic energy t_0, and interactions v_{0i} with the nucleons. Because of Galilean invariance, the total center-of-mass momentum $\mathscr{P}$ is an irrelevant degree of freedom and the scattering wave function should be calculated in terms of N Jacobi coordinates only, namely

$$\pi_0=M^{-1}\left[Nm\mathbf{p}_0-m_0\sum_{i=1}^{N}\mathbf{p}_i\right], \tag{1.1}$$

where π_0 is obviously the relative momentum between the projectile and the center of mass of the target (with m_0, m, and M the projectile, nucleon, and total masses, respectively), and $N-1$ additional Jacobi momenta, such as

$$\pi_1=N^{-1}\left[(N-1)\mathbf{p}_1-\sum_{i=2}^{N}\mathbf{p}_i\right], \tag{1.2}$$

which is the momentum between nucleon 1 and the rest of the target.

The lack of symmetry in the definition of $\pi_1,\pi_2,\ldots,\pi_{N-1}$ is a well known difficulty to be faced[1] when antisymmetrization of the target is at stake. For large values of N the Jacobi representation of exchange is clearly cumbersome. Consequently, one must return to the degrees of freedom $\mathbf{p}_i$, whose single particle nature makes them more convenient variables.

The use of $\mathbf{p}_i$, however, reinstates one superfluous degree of freedom, for there is one more $\mathbf{p}$ than π, and plagues the theory with the well known problem of shell-model spurious states. Despite this difficulty the importance of Pauli-blocking effects in nuclear collisions is so well recognized[2] that we advocate in this paper an antisymmetrized collision theory which is entirely based on shell-model techniques. As will be shown, the existence of a superfluous degree of freedom will not be critical at all. On the contrary, it can be related to quantum recoils which will be used in the theory as dynamical variables.

Section II of this paper explains the basis of wave functions we will use and Sec. III introduces a variational principle for the calculation of recoil effects. Section IV provides a numerical application. Section V is a generalization to the case when the projectile is also a nucleus, and not a structureless particle. Finally, Sec. VI contains a discussion and conclusions.

II. BOOSTED SHELL MODEL BASIS

Let O be the origin of an arbitrary, Galilean reference frame. The momenta $\mathbf{p}_0,\mathbf{p}_1,\ldots,\mathbf{p}_N$ are defined in that frame, and we shall use a set of shell model orbitals constructed around O.

We are interested in particular in nonspurious wave functions of the target, $\psi_n(\mathbf{p}_1,\ldots,\mathbf{p}_N)$, where n is the ordering label in the spectrum of the target. For the sake of simplicity this section deals only with elastic or inelastic scattering, leaving generalizations to Sec. V. We shall also only consider the case in which the projectile is distinguishable from the target nucleons. Our definition[3] of a nonspurious wave function is that ψ_n must factorize as a product of an internal wave function $\psi_n^{\text{int}}(\pi_1,\ldots,\pi_{N-1})$ and a center-of-mass wave function $\gamma(\mathbf{P})$, where $\mathbf{P}=\sum_{i=1}^{N}\mathbf{p}_i$. There are many ways to check whether this factorization is present in actual shell model wave functions without using the Jacobi coordinates, but using the microscopic variables $\mathbf{p}_i$ only. There are also many ways to project partly spurious, shell-model states on purely factorized states if necessary. In any case, we assume in the following that the target center-of-mass wave function is a Gaussian wave packet

$$\gamma(\mathbf{P})=\pi^{-3/4}N^{-3/4}b^{3/2}\exp(-\tfrac{1}{2}N^{-1}b^2P^2), \tag{2.1}$$

where b is the single-nucleon shell model length. The factorization of γ is trivially obtained under standard precautions in the harmonic shell model.

The boosted shell-model state[4] is

$$|\psi_{n,-k}\rangle \equiv \exp(-i\mathbf{k}\cdot\mathbf{R})\,|\psi_n\rangle\ , \tag{2.2}$$

where $\mathbf{k}$ is a parameter vector and the operator $\mathbf{R}=N^{-1}\sum_{i=1}^{N}\mathbf{r}_i$ is just the center-of-mass coordinate of the target. It obviously also factorizes as

$$\psi_{n,-k}(\mathbf{p}_1,\ldots,\mathbf{p}_N)\equiv\langle \mathbf{P}\pi_1,\ldots,\pi_{N-1}\,|\,\psi_{n,-k}\rangle = \gamma(\mathbf{P}+\mathbf{k})\psi_n^{\rm int}(\pi_1,\ldots,\pi_{N-1})\ . \tag{2.3}$$

It must be stressed here that the recoil of ψ_n does not complicate the shell model nature of ψ_n in the macroscopic representation $\{\mathbf{p}_i\}$, because $\exp(-i\mathbf{k}\cdot\mathbf{R})$ is the exponential of a one-body operator. Hence the orbitals contained in the Slater determinants that constitute ψ_n are just boosted by the amount $-N^{-1}\mathbf{k}$. The shell-model expansion of ψ_n in terms of these boosted Slater determinants remains the same.

Consider now the "channel" state $|\mathcal{X}\rangle$ defined by the wave function

$$\langle \mathbf{p}_0,\mathbf{p}_1,\ldots,\mathbf{p}_N\,|\,\mathcal{X}\rangle = \pi^{-3/4}(m_0/m)^{-3/4}b^{3/2} \times\exp[-\tfrac{1}{2}mm_0^{-1}b^2(\mathbf{p}_0-\mathbf{k})^2] \times\psi_{n,-k}(\mathbf{p}_1,\ldots,\mathbf{p}_N)\ . \tag{2.4}$$

Using Eqs. (2.3) and (2.1) and introducing the total center-of-mass (c.m.) momentum $\mathcal{P}=\mathbf{p}_0+\mathbf{P}$, we obtain from Eq. (2.4) the factorization

$$\langle \mathcal{P}\pi_0,\ldots,\pi_{N-1}\,|\,\mathcal{X}\rangle = \gamma_M(\mathcal{P})\gamma_r(\pi_0-\mathbf{k}) \times\psi_n^{\rm int}(\pi_1,\ldots,\pi_{N-1})\ , \tag{2.5}$$

where

$$\gamma_M(\mathcal{P})=\pi^{-3/4}(M/m)^{-3/4}b^{3/2}\exp(-\tfrac{1}{2}mM^{-1}b^2\mathcal{P}^2) \tag{2.6}$$

and

$$\gamma_r(\pi_0-\mathbf{k})=\pi^{-3/4}(\mu/m)^{-3/4}b^{3/2} \times\exp[-\tfrac{1}{2}m\mu^{-1}b^2(\pi_0-\mathbf{k})^2]\ , \tag{2.7}$$

with μ being the projectile-target reduced mass. The γ_M and γ_r indicate, respectively, that the total c.m. is on the average at rest and the projectile-target relative wave function is peaked around $\mathbf{k}$.

A traditional channel wave function $\widetilde{\mathcal{X}}_{nq}$ with momentum $\mathbf{q}$ and unit flux would read, keeping in mind the fact that the total center-of-mass wave function can be frozen arbitrarily,

$$\langle \mathcal{P}\pi_0,\pi_1,\ldots,\pi_{N-1}\,|\,\widetilde{\mathcal{X}}_{nq}\rangle = \gamma_M(\mathcal{P})(2\pi)^{3/2}\delta(\pi_0-\mathbf{q}) \times\psi_n^{\rm int}(\pi_1,\ldots,\pi_{N-1})\ . \tag{2.8}$$

Consider now the Hamiltonian $H=H_0+V$ with $H_0=\mathcal{T}+W$ and

$$\mathcal{T}=t_0+\sum_{i=1}^{N}t_i-\tfrac{1}{2}M^{-1}\mathcal{P}^2\ , \tag{2.9}$$

$$W=\sum_{i>j=1}^{N}w_{ij}\ , \tag{2.10}$$

$$V=\sum_{i=1}^{N}v_{0i}\ . \tag{2.11}$$

The collision amplitude between channels n and n' with momenta $\mathbf{q}$ and $\mathbf{q}'$ is the usual T-matrix element

$$T_{n'n}(\mathbf{q}',\mathbf{q})=\langle\widetilde{\mathcal{X}}_{n'q'}\,|\,[V+V(E^+-H)^{-1}V]\,|\,\widetilde{\mathcal{X}}_{nq}\rangle\ . \tag{2.12}$$

It will be noticed that, since the center of mass has been subtracted from the kinetic energy $\mathcal{T}$, see Eq. (2.9), center-of-mass integrals amount to a unit overlap in Eq. (2.12). Consider now the similar matrix element

$$\mathcal{D}_{n'n}(\mathbf{k}',\mathbf{k})=\langle\mathcal{X}'\,|\,[V+V(E^+-H)^{-1}V]\,|\,\mathcal{X}\rangle\ , \tag{2.13}$$

where $\mathcal{X}'$ is defined like $\mathcal{X}$, Eq. (2.4), with a channel quantum number n' and momentum boost $\mathbf{k}'$. With the aid of Eqs. (2.8) and (2.5) we can rewrite Eq. (2.13) as

$$\langle\mathcal{X}'\,|\,[V+V(E^+-H)^{-1}V]\,|\,\mathcal{X}\rangle = (2\pi)^{-3}\int dq\,dq'\gamma_r(\mathbf{q}'-\mathbf{k}')T_{n'n}(\mathbf{q}',\mathbf{q})\gamma_r(\mathbf{q}-\mathbf{k})\ , \tag{2.14a}$$

or the inverse relation,

$$T_{n'n}(\mathbf{q}',\mathbf{q})=(2\pi)^{-3}\int d\mathbf{k}'d\mathbf{k}\gamma_r^{-1}(\mathbf{q}'-\mathbf{k}') \times\mathcal{D}_{n'n}(\mathbf{k}',\mathbf{k})\gamma_r^{-1}(\mathbf{q}-\mathbf{k})\ , \tag{2.14b}$$

where γ_r^{-1} is the deconvolution kernel related to γ_r.

This result, Eqs. (2.14), is the main result of our choice of a boosted shell model representation. It shows that a T-matrix element can be written as the superposition of amplitudes $\mathcal{D}$ between states $\mathcal{X}$ and $\mathcal{X}'$, which can be calculated in terms of microscopic coordinates $\mathbf{p}_0,\mathbf{p}_1,\ldots,\mathbf{p}_N$. The states $\mathcal{X}$ and $\mathcal{X}'$ therefore behave as representation states, parametrized by the recoil momentum, through which the calculation of the collision proceeds.

The next section provides a variational calculation of $\mathcal{D}$ through shell model techniques and actually takes advantage of recoil as a variational parameter.

III. VARIATIONAL CALCULATION OF RECOIL EFFECTS

In this section we discard from $\mathcal{D}$ the Born term $\langle\mathcal{X}'\,|\,V\,|\,\mathcal{X}\rangle$, which is trivial to calculate, and rather define $\mathcal{D}$ as the matrix element $\langle\mathcal{X}'\,|\,VGV\,|\,\mathcal{X}\rangle$, where G is the Green's function. For the sake of numerical convenience the imaginary part of E will first be taken as finite, thus making G a bounded operator. The on-shell limit will be taken at the end.

Let $\phi(\mathbf{p}_0,\mathbf{p}_1,\ldots,\mathbf{p}_N)$ and $\phi'(\mathbf{p}_0,\ldots,\mathbf{p}_N)$ be two arbitrary trial functions, infinitely flexible at first. An elementary argument of variational calculus shows that the stationary value with respect to ϕ and ϕ' of the functional[5]

$$F=\frac{\langle\mathcal{X}'\,|\,V\,|\,\phi\rangle\langle\phi'\,|\,V\,|\,\mathcal{X}\rangle}{\langle\phi'\,|\,(E-H)\,|\,\phi\rangle} \tag{3.1}$$

is reached when

$$|\phi\rangle=\lambda GV|\chi\rangle,\quad \langle\phi'|=\lambda'\langle\chi'|VG\ , \tag{3.2}$$

where λ and λ' are arbitrary, complex scalars. This stationary value is then nothing but $F^{\rm st}=\langle\chi'|VGV|\chi\rangle$.

It is then interesting to parametrize $\mathscr{D}$ as the result of an entrance width Γ, from χ to an "entrance" doorway state ϕ', then a propagation from ϕ' to an "exit doorway" state ϕ via the "propagator" $\langle\phi'|(E-H)|\phi\rangle^{-1}$, and finally an exit width Γ' from the "exit doorway" state ϕ to the final state χ'. This interpretation is transparent from reading Eq. (3.1).

In a practical case ϕ and ϕ' will be restricted to some subspace of a boosted shell-model basis. Let $\mathbf{K}$ and $\mathbf{K}'$ be boost parameters for ϕ and ϕ', respectively. The stationarity of F with respect to $\mathbf{K},\mathbf{K}'$ is obtained by straightforward derivations of F,

$$\frac{1}{\langle\phi'|V|\chi\rangle}\nabla_{K'}\langle\phi'|V|\chi\rangle - \frac{1}{\langle\phi'|(E-H)|\phi\rangle}\nabla_{K'}\langle\phi'|(E-H)|\phi\rangle=0\ , \tag{3.3a}$$

$$\frac{1}{\langle\chi'|V|\phi\rangle}\nabla_{K}\langle\chi'|V|\phi\rangle - \frac{1}{\langle\phi'|(E-H)|\phi\rangle}\nabla_{K}\langle\phi'|(E-H)|\phi\rangle=0\ . \tag{3.3b}$$

[It can be seen again in Eqs. (3.3) that the norms and phases of ϕ,ϕ' are arbitrary.]

The simplest ansatz for trial functions to be inserted inside F is to take ϕ like χ, Eq. (2.4), with the given boost label $\mathbf{k}$ replaced by a variable boost label $\mathbf{K}$. In the same way, we can take ϕ' as χ', with a variable boost label $\mathbf{K}'$ rather than the final momentum $\mathbf{k}'$. This will provide an approximate $\overline{\mathscr{D}}$ to $\langle\chi'|VGV|\chi\rangle$. The quality of this approximation will be good if the intermediate states of the collision belong to the elastic channel. It is a reasonable assumption when the projectile and target have few excited states, with a large spreading.

Since E is complex, and the on-shell limit actually remains complex because of the $-i\pi\delta(E-H)$ contribution to the propagator, the solution of Eqs. (3.3) must be searched with *complex* values of $\mathbf{K},\mathbf{K}'$. This raises an interesting consequence. While $\mathbf{k},\mathbf{k}'$ are real and thus the wave packets of the projectile and target are on top of each other in coordinate representation, complex values of $\mathbf{K},\mathbf{K}'$ induce both a boost and a shift for the entrance doorway and exit doorway states ϕ',ϕ.

This is seen readily from Eq. (2.7) when the real and imaginary parts of the boost labels are separated:

$$\begin{aligned}\gamma_r(\pi_0-\mathbf{K})=&\pi^{-3/2}(\mu/m)^{-3/4}b^{3/2}\\ &\times\exp[+\tfrac{1}{2}m\mu^{-1}b^2(\mathrm{Im}\mathbf{K})^2]\\ &\times\exp\{-\tfrac{1}{2}m\mu^{-1}b^2[(\pi_0-\mathrm{Re}\mathbf{K})^2\\ &\qquad-2i\,\mathrm{Im}K(\pi_0-\mathrm{Re}\mathbf{K})]\}.\end{aligned} \tag{3.4}$$

The real part of $\mathbf{K}$ corresponds again to a boost, while $\mathrm{Im}\mathbf{K}$ introduces a (nonessential) normalization factor and, more importantly, an oscillatory phase. This phase corresponds to a nonvanishing average value of the relative distance between projectile and target. The entrance doorway and exit doorway solutions of Eqs. (3.3) imply, therefore, a semiclassical impact parameter, and provide at once an estimate of the dominant partial waves for the transition from momentum $\mathbf{k}$ to momentum $\mathbf{k}'$.

While the infinitely flexible variation, Eq. (3.2), corresponds to a linear problem, the present restriction of trial functions to frozen states with just a recoil parameter is now a nonlinear approximation. Hence, Eqs. (3.3) may have more than one solution. Nothing prevents us in a future stage of the theory from mixing these solutions linearly through the ansatz

$$\phi=\sum_\nu C_\nu\phi_\nu,\quad \phi'=\sum_\nu C'_\nu\phi'_\nu\ , \tag{3.5}$$

where ν is the label for these various recoils $\mathbf{K}_\nu,\mathbf{K}'_\nu$. The mixture coefficients C_ν,C'_ν then induce an interference between the various mechanisms (partial waves, semiclassical trajectories) represented by ϕ_ν,ϕ'_ν.

To conclude this section it must be stressed that recoiling shell-model nuclear wave functions can be used as dynamical intermediate states in a theory of collisions. In the next section we shall investigate numerically the solution of Eqs. (3.3) in a case where nuclear structure is the simplest possible case; namely, ψ_{nk} is reduced to just one Slater determinant.

IV. AN ILLUSTRATIVE EXAMPLE

We consider here the $\mathscr{D}$ for an elastic collision of a meson and an α particle, the structure of the latter being approximated by just a $(0s)^4$ wave function, in a spherical harmonic oscillator, and antisymmetrization of the target being taken care of by a Slater determinant of spin and isospin variables. The meson-nucleon interaction v is taken as central, spin, and isospin independent,

$$\langle\mathbf{p}'_0\mathbf{p}'_i|v|\mathbf{p}_0\mathbf{p}_i\rangle=\lambda_0\delta(\mathbf{p}'_0+\mathbf{p}'_i-\mathbf{p}_0-\mathbf{p}_i)\frac{m\mathbf{p}'_0-m_0\mathbf{p}'_i}{m+m_0}\cdot\frac{m\mathbf{p}_0-m_0\mathbf{p}_i}{m+m_0}\exp\left\{-\frac{\nu^2[(m\mathbf{p}'_0-m_0\mathbf{p}'_i)^2+(m\mathbf{p}_0-m_0\mathbf{p}_i)^2]}{(m+m_0)^2}\right\}. \tag{4.1}$$

Hence the spin-isospin determinant will be understood in the following. All the wave functions considered in this section have the form

$$\begin{aligned}\langle\mathbf{p}_0\mathbf{p}_1\mathbf{p}_2\mathbf{p}_3\mathbf{p}_4|\mathbf{k}\rangle=&\pi^{-3/4}(m_0/m)^{-3/4}b^{3/2}\exp[-\tfrac{1}{2}mm_0^{-1}b^2(\mathbf{p}_0-\mathbf{k})^2]\\ &\times\pi^{-3}b^6\exp\left\{-\tfrac{1}{2}b^2\left[\left(\mathbf{p}_1+\frac{k}{4}\right)^2+\left(\mathbf{p}_2+\frac{k}{4}\right)^2+\left(\mathbf{p}_3+\frac{k}{4}\right)^2+\left(\mathbf{p}_4+\frac{k}{4}\right)^2\right]\right\};\end{aligned} \tag{4.2}$$

namely, $\mathbf{k}$ will be just replaced by $\mathbf{k}'$, $\mathbf{K}$, and $\mathbf{K}'$ when we define χ', ϕ, and ϕ', respectively. In other words, we restrict the collision to the elastic channel and the trial functions to the elastic channel also.

A straightforward calculation then gives

$$F(\mathbf{k}',\mathbf{k},\mathbf{K}',\mathbf{K})=\frac{\langle\mathbf{K}'\,|\,V\,|\,\mathbf{k}\rangle\langle\mathbf{k}'\,|\,V\,|\,\mathbf{K}\rangle}{-\langle\mathbf{K}'\,|\,V\,|\,\mathbf{K}\rangle+\langle\mathbf{K}'\,|\,(E-H_0)\,|\,\mathbf{K}\rangle}=\frac{f(\mathbf{K}',\mathbf{k})f(\mathbf{k}',\mathbf{K})}{-f(\mathbf{K}',\mathbf{K})+g(\mathbf{K}',\mathbf{K})}\ , \tag{4.3}$$

with

$$f(\mathbf{K}',\mathbf{K})=\Lambda\mathbf{K}\cdot\mathbf{K}'^{*}\exp\{-[a_1(\mathbf{K}^2+\mathbf{K}'^{*2})+a_2(\mathbf{K}-\mathbf{K}'^{*})^2]\}\ , \tag{4.4}$$

$$g(\mathbf{K}',\mathbf{K})=\left[E-E_\alpha-\frac{3\hbar^2}{4mb^2}-a_3(\mathbf{K}+\mathbf{K}'^{*})^2\right]\times\exp\{-[a_4(\mathbf{K}-\mathbf{K}'^{*})^2]\}\ , \tag{4.5}$$

where E_α is the internal energy of the target and takes care of the constant matrix element of W since only elastic wave functions are included. We have defined

$$\Lambda=4\lambda_0\pi^{3/2}b^3\beta^4(\beta^2+\nu^2)^{-5}(1+\tfrac{1}{4}m_0/m)^2\times(1+m_0/m)^{-1/2}(m_0/m)^{-3/2}\ , \tag{4.6}$$

$$\beta^2=\frac{b^2(1+m_0/m)}{2m_0/m}\ , \tag{4.7}$$

$$a_1=\beta^2\nu^2(1+\tfrac{1}{4}m_0/m)^2(1+m_0/m)^{-2}(\beta^2+\nu^2)^{-1}\ , \tag{4.8}$$

$$a_2=\frac{3b^2}{64}\left[\frac{3}{1+m_0/m}+1\right]\ , \tag{4.9}$$

$$a_3=\frac{\hbar^2}{2m}\frac{4+m_0/m}{16m_0/m}\ , \tag{4.10}$$

$$a_4=b^2\frac{4+m_0/m}{16m_0/m}\ . \tag{4.11}$$

It is trivial to take derivatives of the symmetric function F, Eq. (4.3), with respect to its arguments $\mathbf{K}$ and $\mathbf{K}'^{*}$. An elementary geometrical argument shows that those vectors $\mathbf{K},\mathbf{K}'$ which cancel the derivatives are in the plane defined by $\mathbf{k}$ and $\mathbf{k}'$; hence only four equations must be solved simultaneously rather than six at first sight.

The variational equations have been solved numerically with the following values of the parameters: $b=1$ fm, $\hbar^2/2m=20$ MeV fm^2, $m_0/m=0.15$, $\lambda_0=-20$ MeV fm^5, and $E_\alpha=-20$ MeV. The code RECLCR is available on request to the interested reader. The search for the solution is initiated forward from a first guess $\mathbf{K}=\mathbf{k}$, $\mathbf{K}'=\mathbf{k}'$; then a path is investigated in the eight-dimensional parameter space (two complex components for each $\mathbf{K},\mathbf{K}'^{*}$) in order to diminish the modulus of the logarithmic derivative of F. Then angles and energies are varied smoothly.

Solutions are found quite rapidly and indeed, at least for small-angle elastic scattering, $\mathbf{K}$ does not differ too much from $\mathbf{k}$, and $\mathbf{K}'$ is not too far from $\mathbf{k}'$. Nonetheless, $\mathbf{K}$ and $\mathbf{K}'$ are complex, as expected. As a general rule their imaginary parts are smaller than their real parts in the energy domain investigated here ($|\mathbf{k}|=|\mathbf{k}'|\simeq 0.1$ to 1.5 fm^{-1}). For Im$E>0$, and small-angle scattering, the signs of the imaginary parts of $\mathbf{K},\mathbf{K}'^{*}$ are dominantly negative and the signs of the imaginary parts of the variational amplitudes $\mathscr{D}$ are also negative.

In the forward direction (case $\mathbf{k}=\mathbf{k}'$), the exact amplitude *must* have an imaginary part with a sign opposite that of E. The variational amplitude also shows the right sign. We also verify that $\mathbf{K}=\mathbf{K}'^{*}$ in that case, a result already established[6] as a property of our variational principle.

We show in Fig. 1 the angular behavior of the variational amplitude when $|\mathbf{k}|=|\mathbf{k}'|=1$ fm^{-1} and Im$E=50$ MeV. A similar angular evolution is shown in Fig. 2 for the same energy (Re$E=118.33$ MeV) but a vanishing ImE. We stress that this on-shell limit of the theory is extremely smooth. In Fig. 2 we also show the forward $\overline{\mathscr{D}}$ when $|\mathbf{k}|=|\mathbf{k}'|$ is raised from 1 to 1.5 fm^{-1}. Then we show in Fig. 3 the values taken by Re$\mathbf{K}'^{*}$ and Im$\mathbf{K}'^{*}$, respectively, for $|\mathbf{k}|=|\mathbf{k}'|=1$ fm^{-1}, Re$E=118.33$ MeV, and Im$E=0$. The vector $\mathbf{K}$ can be deduced from the vector $\mathbf{K}'^{*}$ via a reflection about the bisector of the angle between $\mathbf{k}$ and $\mathbf{k}'$, an obvious symmetry of the problem. Finally, in Fig. 4 we show the angular distribution of the variational cross section when $|\mathbf{k}|=|\mathbf{k}'|=1.5$ fm^{-1} and Im$E=0$. The Born term has been reinstated and wave packets have been renormalized to unit flux at the shell model center, as in Ref. 7. The smooth behavior of all these quantities brings no evidence of singularities such as bifurcations in our nonlinear approximation. All these results are average results and correspond to Eq. (2.13), the amplitude between wave packets. The deconvolution described by Eq. (2.14b) is now under study.

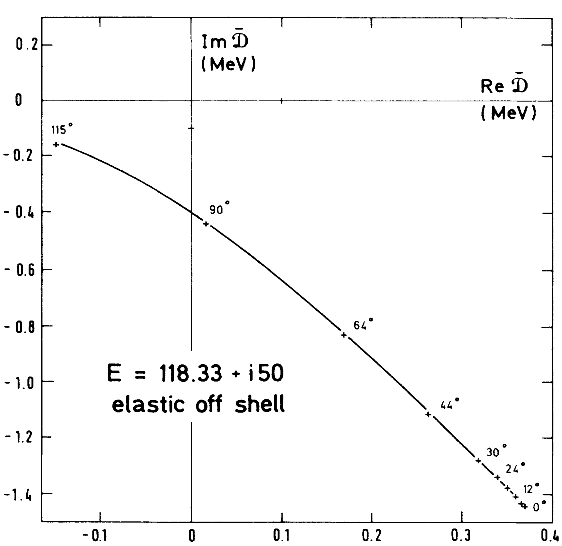

FIG. 1. Angular behavior of the multistep amplitude $\overline{\mathscr{D}}\simeq\langle\chi'\,|\,VGV\,|\,\chi\rangle$ provided by the model. The energy is off shell, $E=118.33+50i$ ($|\mathbf{k}|=|\mathbf{k}'|=1$ fm^{-1}). For the other parameters, see the text.

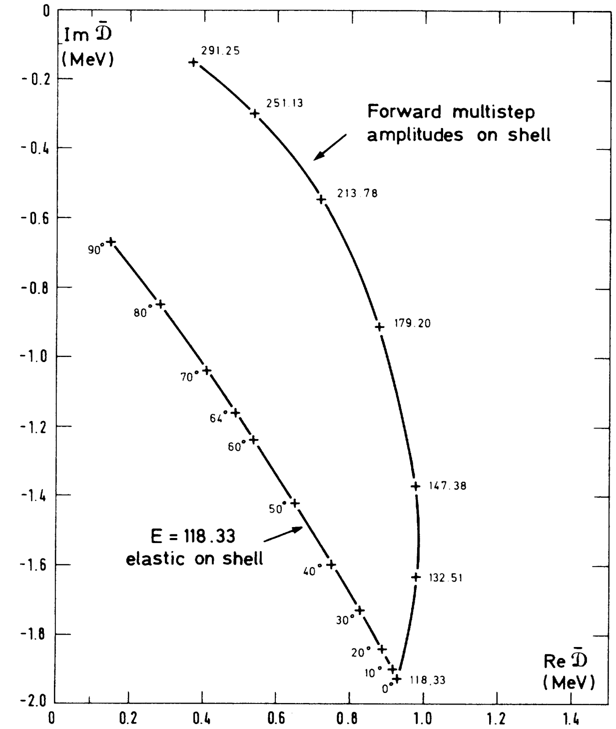

FIG. 2. Left-hand branch same as for Fig. 1, but on shell (Im$E=0$). Right-hand branch shows the on-shell forward amplitude $\overline{\mathscr{D}}$ when $\mathbf{k}=\mathbf{k}'$ and $|\mathbf{k}|$ rises from 1.0 to 1.5 fm^{-1}.

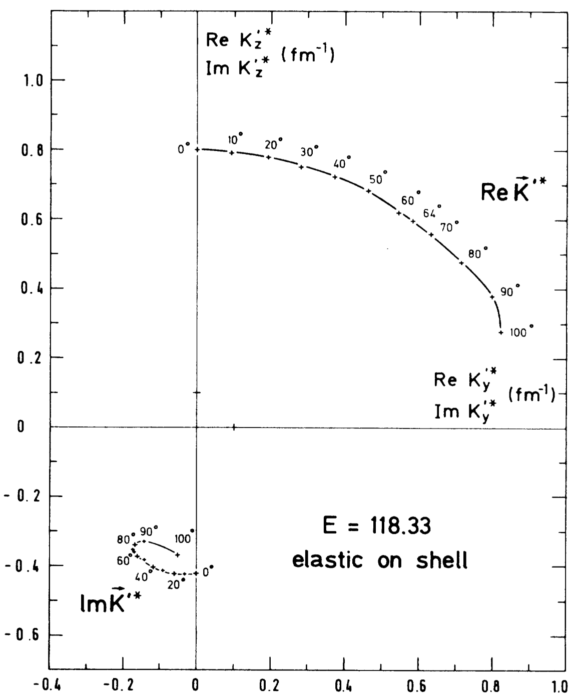

FIG. 3. Angular behavior of Re$\mathbf{K}'^*$ (top branch) and Im$\mathbf{K}'^*$ (bottom branch) when $|\mathbf{k}|=|\mathbf{k}'|=1$ fm^{-1} and E is on shell. The angle shown besides each point is the scattering angle between $\mathbf{k}$ and $\mathbf{k}'$. To obtain $\mathbf{K}$ take the symmetric of $\mathbf{K}'^*$ with respect to the bisector of $\mathbf{k},\mathbf{k}'$. We have chosen the reaction plane as the (y,z) plane, with the initial momentum $\mathbf{k}$ along the z axis.

V. GENERALIZATION

The obvious generalization of Eq. (2.4) when a channel contains a composite projectile a and a target A is obviously

$$\langle \mathbf{p}_1,\mathbf{p}_2,\ldots,\mathbf{p}_a,\mathbf{p}_{a+1},\ldots,\mathbf{p}_{A+a}\,|\,\chi\rangle=\mathscr{A}\psi^{(a)}_{n_1,k}\psi^{(A)}_{n_2,-k}\ , \tag{5.1}$$

where $\mathscr{A}$ is the total antisymmetrizer. Here $\psi^{(a)}_{n_1}$ is the static shell model wave function $\psi^{(a)}_{n_1}(\mathbf{p}_1,\ldots,\mathbf{p}_a)$ of nucleus a in quantum state n_1, and it must factorize as a product of an internal wave function $\psi^{(a)\mathrm{int}}_{n_1}(\pi_1,\ldots,\pi_{a-1})$ and a center-of-mass wave packet

$$\gamma_a(\mathbf{P}_a)=\pi^{-3/4}(M_a)^{-3/4}b^{3/2}\exp(-\tfrac{1}{2}b^2M_a^{-1}P_a^2)\ , \tag{5.2}$$

where $\pi_1,\ldots,\pi_{a-1}$ are the Jacobi momenta internal to nucleus a, then $\mathbf{P}_a$ is its center-of-mass momentum, and M_a is its mass number. A momentum boost $\mathbf{k}$ converts $\psi^{(a)}_{n_1}$ into

$$\psi^{(a)}_{n_1,k}=\exp(i\mathbf{k}\cdot\mathbf{R}_a)\psi^{(a)}_{n_1}\ , \tag{5.3}$$

where $\mathbf{R}_a$ is the conjugate of $\mathbf{P}_a$ and just boosts the individual single particle orbitals contained in $\psi^{(a)}_{n_1}$. This leaves the factorization of $\psi^{(a)\mathrm{int}}_{n_1}$ unaltered and generates a c.m. wave packet

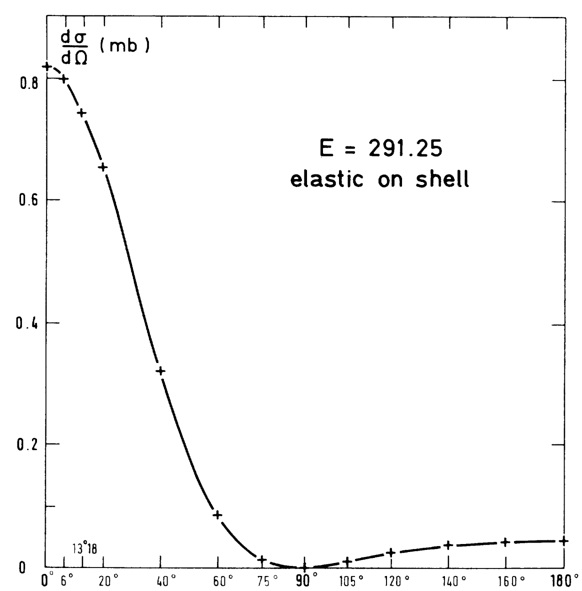

FIG. 4. Complete angular distribution, including the Born term, provided by the model for elastic scattering at $|\mathbf{k}|=1.5$ fm^{-1} and E on shell.

$$\gamma_a(\mathbf{P}_a-\mathbf{k})=\pi^{-3/4}(M_a)^{-3/4}b^{3/2}\times\exp[-\tfrac{1}{2}b^2M_a^{-1}(\mathbf{P}_a-\mathbf{k})^2]\ . \tag{5.4}$$

As to $\psi^{(A)}_{n_2,-k}$, a completely similar argument defines it as the product of an internal wave function $\psi^{(A)}_{n_1}(\pi_{a+1},\ldots,\pi_{A+a-1})$ and a center-of-mass wave packet

$$\gamma_A(\mathbf{P}_A+\mathbf{k})=\pi^{-3/4}(M_A)^{-3/4}b^{3/2}\times\exp[-\tfrac{1}{2}b^2M_a^{-1}(\mathbf{P}_A+\mathbf{k})^2]\ . \tag{5.5}$$

The relative motion and total c.m. wave packets are then derived from the product of Eqs. (5.4) and (5.5), expressed in terms of the total c.m. and relative momenta $\mathscr{P}=\mathbf{P}_a+\mathbf{P}_A$ and $\mathbf{p}=(M_A\mathbf{P}_a-M_a\mathbf{P}_A)/(M_a+M_A)$, respectively,

$$\chi=\pi^{-3/4}(M_a+M_A)^{-3/4}b^{3/2}\exp[-\tfrac{1}{2}b^2(M_a+M_A)^{-1}\mathscr{P}^2]\mathscr{A}\pi^{-3/4}\left[\frac{M_aM_A}{M_a+M_A}\right]^{-3/4}b^{3/2}$$
$$\times\exp\left[-\tfrac{1}{2}b^2\frac{M_a+M_A}{M_aM_A}(\mathbf{p}-\mathbf{k})^2\right]\psi^{(a)\text{int}}_{n_1}(\pi_1,\ldots,\pi_{a-1})\psi^{(A)\text{int}}_{n_2}(\pi_{a+1},\ldots,\pi_{A+a-1})\ . \tag{5.6}$$

It is clear from Eq. (5.6) that the total center of mass is at rest on the average, while the relative momentum peaks around $\mathbf{k}$ and the internal structures are specified by the channel label pair (n_1n_2). It must be stressed again here that, although the physical content of χ is more transparent in terms of Jacobi coordinates in Eq. (5.6), the product defined by Eq. (5.1) can be expressed in second quantization as a product of boosted single-particle creation operators generating $\psi^{(a)}_{n_1,k}$ and $\psi^{(A)}_{n_2,-k}$.

The generalization to three-or-more-fragment channels is obvious; for instance,

$$\chi=\mathscr{A}\psi^{(a)}_{n_1,\mathbf{k}_1}\psi^{(b)}_{n_2,\mathbf{k}_2}\psi^{(c)}_{n_3,\mathbf{k}_3}\ , \tag{5.7}$$

with $\mathbf{k}_1+\mathbf{k}_2+\mathbf{k}_3=0$. Trial functions can be of the form Eq. (5.1) or Eq. (5.7), with variable labels $\mathbf{K}$ rather than fixed labels $\mathbf{k}$.

VI. DISCUSSION AND CONCLUSIONS

For spectroscopic calculations, a recoiling wave function $\psi_{n,-k}$, Eq. (2.2), is regarded as spurious, in the sense that the only relevant dynamics, which is the internal dynamics, is Galilean invariant. In the presence of another wave function, however, which is boosted in the opposite direction, such as the projectile wave packet in Eq. (2.4), the boost label is tantamount to a Jacobi momentum of the composite projectile-target system. This is clearly seen, for instance, in Eq. (2.5), where $\mathbf{k}$ is the mean value of π_0, or in Eq. (5.6), where it is the mean value of $\mathbf{p}$.

Hence these recoil labels can be used as dynamical parameters in the calculation of a collision amplitude. As illustrated in Sec. IV, it is very practical to calculate matrix elements in a microscopic representation with single particle coordinates $\{\mathbf{p}_i\}$, and to use the boost labels as variational parameters. The simplicity of the manipulation of multicluster channels, see Eq. (5.7), shows that the method may have a wide range of applications.

Besides allowing an easy antisymmetrization and taking properly into account center-of-mass effects, the method shows an extremely striking result, namely its smooth on-shell limit. Even though the functional F, Eq. (3.1), is formally real when $\text{Im}E=0$, our approximation spontaneously breaks time reversal invariance. The *complex* solution $\mathbf{K},\mathbf{K}'$ which provides the results plotted in Figs. 1–4 is actually not the only one: there is a conjugate solution $\mathbf{K}^*,\mathbf{K}'^*$; hence time reversal is globally restored. The reason we chose the first rather than the second solution is twofold; namely, (i) the first solution emerges naturally as the nearest and most stable solution in the vicinity of $\mathbf{k},\mathbf{k}'$ when $\text{Im}E>0$, and (ii) this solution provides the correct sign of the forward, retarded scattering amplitude. Future refinements of the theory are possible if additional pairs of conjugate solutions are discovered. The results obtained in this paper at the time being are sufficient by themselves to claim that we have a theory of collisions which is regular on shell, a nontrivial result.

Last but not least, the orders of magnitude and angular trends of the cross sections provided by the theory are very reasonable. With only a very schematic π-N interaction and a rigid α structure, we obtain millibarns or tenths of millibarns, with a smooth decrease from forward to backward angles. No variation of parameters to balance the Born term against the multistep amplitude $\langle\chi'\mid VGV\mid\chi\rangle$ has been attempted. The only problem left open by the present paper, besides of course an extension of the flexibility of trial functions, is the deconvolution demanded by Eq. (2.14b). This is now under investigation.

It can be concluded that we have reached a practical stage in this microscopic theory of collisions.

ACKNOWLEDGMENTS

Part of this work was supported by NATO Grant 606/84. The hospitality of Los Alamos Laboratories, Group INC11, is acknowledged by one of us (B.G.G.). The hospitality of Service de Physique Théorique, Saclay, is also acknowledged by two of us (S.K. and L.C.L.) with great pleasure. It is also a pleasure to thank T. Sami for a stimulating discussion on the possible relation between this model and the time-dependent cluster model.[8]

[1]L. C. Liu and C. M. Shakin, Nuovo Cimento **53A**, 142 (1979).
[2]W. B. Kaufmann and W. R. Gibbs, Phys. Rev. C **28**, 1286 (1983).
[3]B. G. Giraud, Nucl. Phys. **11**, 373 (1965).
[4]B. G. Giraud and M. A. Nagarajan, J. Phys. (Paris) **41**, 477 (1980).
[5]B. G. Giraud and M. A. Nagarajan, J. Phys. G **4**, 1739 (1978).
[6]P. Amiot, B. G. Giraud, and M. A. Nagarajan, Phys. Rev. C **29**, 2374 (1984).
[7]B. G. Giraud and M. A. Nagarajan, Phys. Rev. C **28**, 1918 (1983).
[8]E Caurier, B. Grammaticos, and T. Sami, Phys. Lett. **109B**, 150 (1982).